IOSR Journal of Applied Physics (IOSR-JAP)
e-ISSN: 2278-4861.Volume 7, Issue 5 Ver. II (Sep. - Oct. 2015), PP 19-32
www.iosrjournals

Spin Resolved Analysis on Electronic Structural Properties of Zinc Oxide Nanosheet Attached to Ni Electrodes with Carbon Sheet for Comparison

S. Yusuf[1]*, S. Caliscan[2]., And A. Marmori[3]
[1]*Department of Physics, Kano University of Science and Technology, Wudil. Kano State, Nigeria.*
[2]*Department of Physics, Fatih University, Buyucekmece Istanbul, Turkey.*
[3]*AI Rwad Academy Amman, Jordan.*

Abstract: *We explored spin dependent electronic structural properties of two dimensional systems in the form of periodic and device structures. As a two dimensional system we mainly focused on ZnO sheets. In addition to ZnO sheets, C sheets were also examined in order to make a comparison in terms of spin dependent electronic structural properties. In the device structures, they were placed between two homogenous ferromagnetic Nickel (Ni) electrodes that helped us to investigate and analyze possible effects concerning the spin dependent behavior or spin polarization. Besides, induced magnetic moment was considered as well to reveal the magnetic properties of these two dimensional systems. In addition to perfect structures, we also studied the effect of distortion and doping atoms introduced in the sheets. It was observed that both the distortion and dopants provided by transition metal atoms have a crucial role on the electronic structural properties. Using ferromagnetic electrodes, distortion and dopants, one can play with spin dependent behavior needed in developing spintronic devices.*

Keywords*: First principles, Density functional theory, ZnO sheet, C sheet, Ferromagnetic electrode, Spin dependent property, device structures.*

I. Introduction

Spin-dependent transport has been a subject of tremendous concerned in today's scientific researches and technologies [1, 2]. When combined successfully with semiconductor functionalities, spin-based electronics or spintronics may have enormous considerable impact on future electronic device applications [3–5]. Spintronics emerged from the discoveries in the 1980s concerning the spin-dependent electron transport phenomena in solid-state devices. These include the observation of spin-polarized electron injection from a ferromagnetic metal to a normal metal [6] and the discovery of giant magneto-resistance [7-8]. In this research, we are concerned with Nanostructures, which are system of intermediate size between microscopic and molecular structures [9]. Nanostructures are composed of different kind of structures such as atomic wires, branched structures, molecular junctions, organic and biological structures, nanosheets etc. Moreover, in nanostructures it is necessary to describe the dimension of the system. Besides, among the nanoscale structures for instance; nanotextured surfaces have one dimension, nanosheets have two dimensions and spherical nanoparticles have three dimensions. Integration of these structures with spintronics leads to useful devices that have multifunctional and superior properties. This integration means analyzing the properties of these systems by involving the spin property of the electrons. Spin is a quantum mechanical property of the electron. It is an intrinsic property of an electron like charge and mass. It arises from the rotation of the electron around itself. Spin property of the electron has become important in addition to its charge. Due to this property, possible devices which specifically exploit the spin property instead of or in addition to the charge were proposed. For example, spin relaxation and spin transport in metals and semiconductors are of fundamental research interest not only for being fundamental solid state physics issues but also for the already demonstrated potential in electronic technology [9-10]. Moreover, this technology leads to revolutionary advancement in the next generation electronics such as ultra fast, high dense memory devices, logics with extremely low power, enhanced functionality of devices, smaller device size as well as faster operation [1]. Current efforts in designing and manufacturing spintronic devices with regard to this technology, involve two different approaches. First effort is perfecting the existing giant magneto resistance (GMR) based technology by either developing new materials with larger spin polarization of electrons or making improvements or variations in the existing devices for better spin filtering [11]. The second one, which is more radical, focuses on finding novel ways of both generation and utilization of spin-polarized currents, which include investigation of spin transport in semiconductors and looks for ways in which semiconductors can function as spin polarizer's and spin valves. The importance of this effort lies in the fact that the existing metal-based devices do not amplify signals, though they are successful switches or valves, whereas semiconductor based spintronic devices could in principle

provide amplification and serve, in general, as multi-functional devices. Perhaps even more importantly, it is much easier for semiconductor-based devices to be integrated with traditional semiconductor technology [12]. Information in general is carried out either by flow of electric charges or movement of spins. In order to convey spin information through a system we need spin polarized electrodes. Spin polarized transport occurs in many materials where one can observe unstable randomized motions in different directions and interaction of spins. The density of states available to spin up and spin down electrons is often matched together due to the ferromagnetic metals encompassed and boosts spintronics devices scientifically and technologically in the semiconductor industries and researches [2]. ZnO sheet is one of the most promising semiconducting materials in recent researches and technologies. ZnO has a wide band gap (3.37 eV) with a large exciton binding energy (60 meV), and exhibits sensational piezoelectric and optical properties [13]. The knowledge about growth direction of a ZnO sheet (Figure 1) helped us enormously in achieving our goals using the software package (ATK) where 1.9 Angstrom (Å) was determined as the lattice constant between a Zinc (Zn) and Oxygen (O) atom.

II. Materials And Methods

In this research, using the various nanosheets, we intended to investigate the spin dependent properties of two dimensional systems attached to ferromagnetic electrodes. Our goal is, in particular, to examine and to reveal the spin dependent properties of ZnO nanosheets by calculating corresponding quantities, such as transmission, density of states, partial density of states, local density of states, conductance, current-voltage characteristics etc. We utilized the software package called Atomistix Toolkit (ATK), which is based on Density Functional Theory (DFT), to analyze the electronic and magnetic properties of two dimensional systems. The numerical methods used in this program are based on first principles. It combines "Non-Equilibrium Green's Function" (NEGF) and "Density Functional Theory" (DFT) which can give the information about the electronic structural properties of a system. During the calculations, ATK solves the quantum mechanical equations describing electronic Properties, through which one can simulate the spin dependent behavior of nanoscale systems. In the present work, especially ZnO sheets are concentrated and compared to other sheets consisting of, for instance, carbon atoms. The ferromagnetic electrodes serving as a source and drain are used to examine the spin dependent transport where electrode-system coupling plays a crucial role. In order to be comparable to the experiments, the systems joining the electrodes should contain the impurities and must be optimized (relaxed) to mimic the realistic devices formed by left electrode-system-right electrode. Thus, we performed DFT calculations through the nanosheets with and without impurities, which were coupled between two Ni electrodes, and investigate the effect of electrodes, impurities and other factors on these structures.

III. Figures

In this section, the geometric configurations of these systems (i.e ZnO and C sheets) are presented. Figure 1, illustrate growth direction and the width of Zinc (Zn) and Oxygen (O) atom, with red and green atom represent O and Zn atom, respectively.

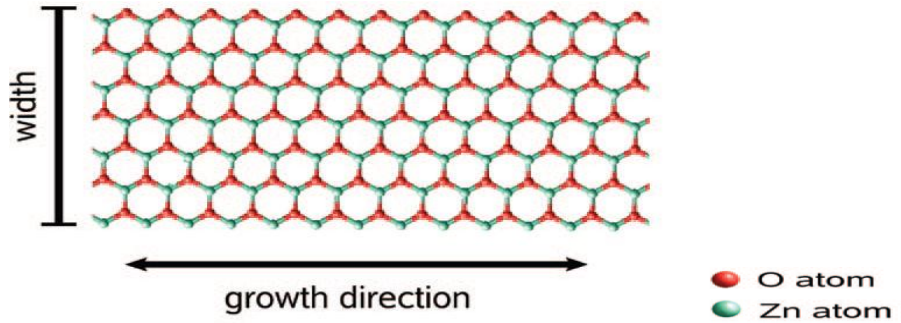

Figure 1: Growth of a ZnO Sheet using ATK. (ATK Ver., 2011).

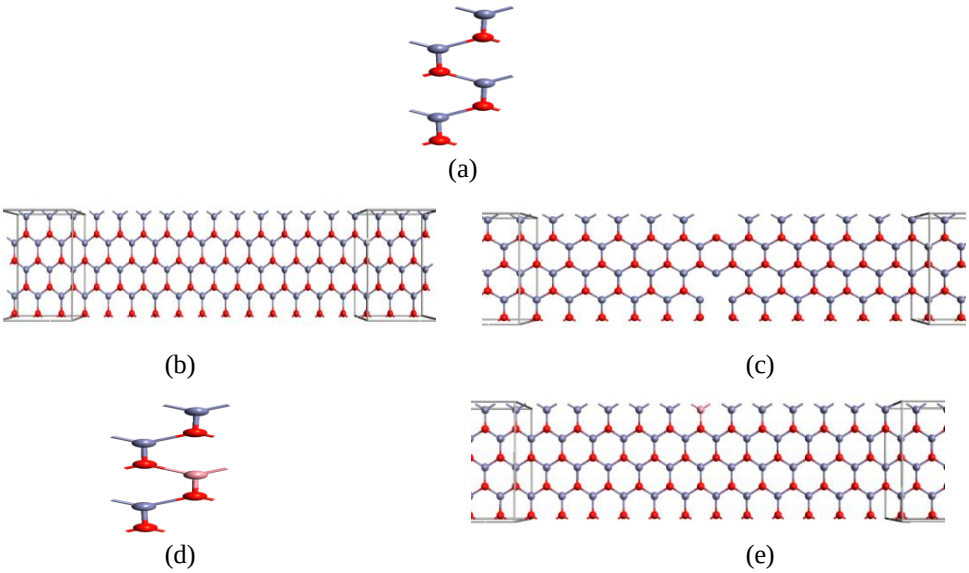

Figure 2: ZnO periodic and device structures (Zn: blue, O: red and Co: pink). (a) ZnO sheet (periodic) (b) ZnO device structure (c) Distorted ZnO device structure (d) Co doped ZnO sheet (periodic) (e) Co doped ZnO device structure. (ATK Ver., 2011).

Figure 2, illustrates the ZnO sheets in the form of periodic and device structures. A ZnO device structure is a two probe system consisting of ZnO sheets, i. e., both the electrodes and central region contain ZnO sheet. ZnO sheets were constructed with eight atoms as seen in Fig. 5.1a which represents the unit cell. Using the sheet in Figure 2a, we have constructed the ZnO device structure. We have introduced both distortions (Figure 2c) via removing atoms and impurity (Figure 2d and e) by means of cobalt (Co) atom which replaces the Zn atom. Co is ferromagnetic and transition metal which can induce magnetic moment or spin polarization in a system. Thus, both the substitutional impurity atom and the distortions in these structures were applied so as to detect any significant effect that might be resulted on spin polarized transport behavior. The effects of spins were also analyzed through ferromagnetic homogeneous nickel (Ni) electrodes. Both Ni and Co are transition elements whose d orbital leads to significant effects on the spin dependent transport and magnetic behavior. For the systems in Fig.5.1b, c, and e we carried out magnetic moment calculation via Mullikan Population analysis to reveal out magnetic behavior of particular device structures [14]. For the system in Figure 2b, the average magnetic moment per central atom was almost zero, implying no spin polarization induced. As for the system in Figure 2c, we observed an average magnetic moment as 0.0296_B (Bohr magnetron) per central atom, arising as a result of distortion. However, for a Co doped ZnO device (Figure 2e), the average magnetic moment was raised to 0.075_B per central atom, which clearly manifests the magnetic behavior of this structure. Hence, for the distorted and transition metal doped ZnO device structure one can obtain spin dependent behavior or spin polarization which can be utilized in the field of spintronics. Energy gap (E_g), density of states (DOS) and transmission spectrum (T(E)) can be altered due to distortion and doping concentration.

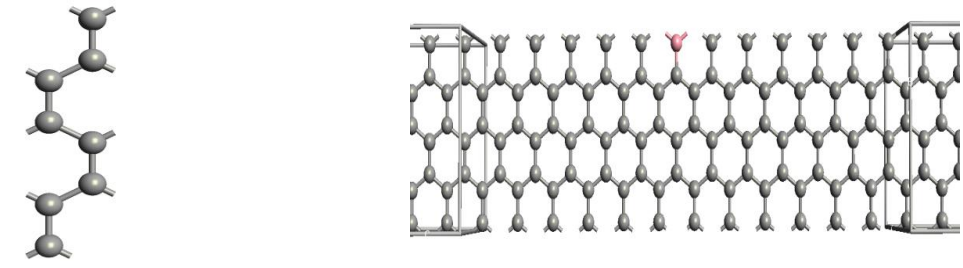

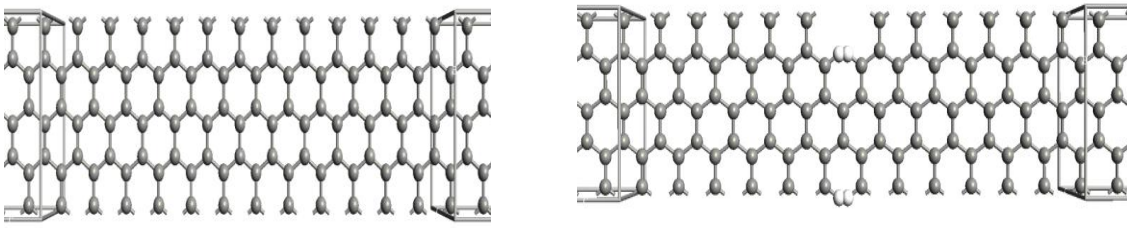

(c) (d)

Figure 3: Carbon sheets in the form of periodic and device structures (C: grey and Co: pink). (a) C sheet (periodic) (b) Co doped C device structure (c) C device structure (d) Distorted C device structure. (ATK Ver., 2011).

Figure 3, illustrates the C sheets in the form of periodic (bulk system) and device structures (open system). C device structure is a two probe system consisting of C sheets, i. e., both the electrodes and central region contain C sheet. As in the case of ZnO based systems, we have introduced both Co impurity (Figure 3b) and distortion (Figure 3d). Distortion was introduced via removing atoms and passivation with hydrogen (H) atoms. Impurity was added through substitutionally replacing Zn atoms by Co. A Co atom induces magnetic moment or spin polarization throughout the system, as mentioned above. Through the magnetic moment calculations, one is able to determine the magnetic properties of the structures in Figure 3. We thought that using the substitutional impurities and/or distortions it could be possible to induce the magnetic moment, resulting in spin polarized transport. However, we determined that the average magnetic moment per central atom in the presence of Co impurity (Figure 3b) was roughly zero due to very low Co concentration compared to total atoms in the device. It was calculated as. As for the perfect C device without impurity in Figure 3c, the average magnetic moment was found as, per central atom, which was substantially reduced when Co impurity was remove.

IV. Results And Dıcussıons

The electronic structural properties (especially band gap, density of state, and transmission spectrum) of different constructed nanosheets (ZnO and Carbon sheets in particular) have been examined, using first principles by DFT calculations. In order to be comparable to the experimental results, different exchange correlations and k-points sampling have been employed. We also involved distortion, impurities in the systems to be more realistic and Hubbard term (U) to enhance the accuracy of the results [15]. It is known that GGA and LDA underestimate the band gap, so one needs to include the correction term U. We have examined transport properties and especially focus on the spin polarized structural properties. Moreover, we have also investigated the magnetic properties through magnetic moment calculations for some specific systems. In numerical calculations we have in general used double zeta polarized basis set, due to its accuracy shown by most practical results and experiences, with GGA approximation. But for some configurations, LDA approximation was also considered for the sake of comparison, even though it might give incorrect results. The parameters such as Brillouin zone integration parameters, k-points sampling, mesh cut-off, initial spin values injected to the central regions, electrode temperature and other self consistent field parameters were also considered. Thus, we observed and analyzed the possible effects on the results for each periodic (bulk system) and device structures (two probe system). In the presented band structure results and spectra, spin up (majority) and spin down (minority) variations are shown by positive (black) and negative (red) values for the sake of clarity.

4.1 Electronic Structural Properties of ZnO Sheet

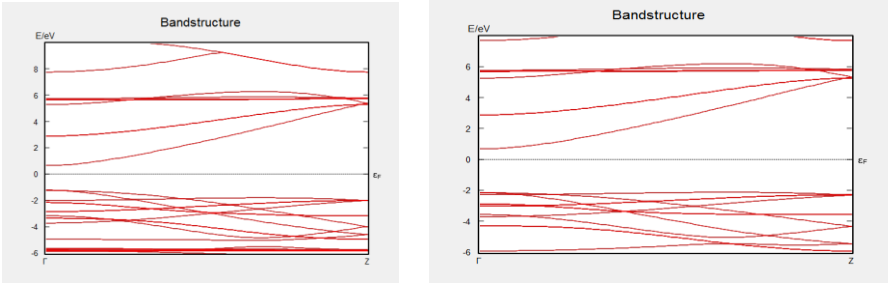

(a) (b)

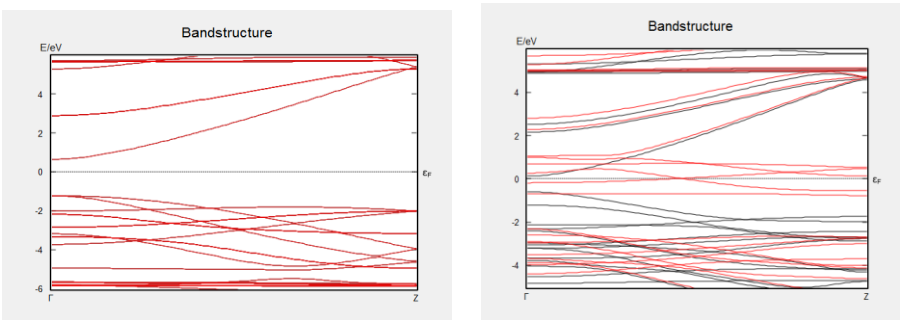

(c) (d)

Figure 4: Band structures for (a) ZnO sheet (b) ZnO sheet with U correction (c) optimized ZnO sheet (d) Co doped ZnO sheet when spin is involved in the calculations.

Figure 4, shows the band structures of ZnO sheets when spin is involved. The zero energy level indicates the Fermi energy (E_f). We see from Figure 4a-c that majority and minority variations in the band structures are identical, meaning they are spin symmetric. Thus, there is no spin dependent variation for the structures in Figure 4a-c and so majority E_g becomes equal to minority E_g. As for the structure in Figure 4d, majority E_g is different from minority E_g, and hence they are spin asymmetric. It means there is a spin dependent variation or spin polarization due to Co doping (Figure 4d). Therefore in a pure perfect ZnO sheet, it is not possible to observe spin dependent energy gap and one needs a transition metal like Co to induce a spin dependent property. The semiconducting behavior was clearly observed for pure ZnO sheets. The E_g value of the pure perfect ZnO sheet was found to be 1.86 eV for both majority and minority spins (Figure 4a). However, upon introducing the correction term U it increased to 2.80 eV, which is more accurate (Figure 4b). The E_g value of the pure optimized perfect ZnO sheet was found to be 1.87 eV for both majority and minority spins (Figure 4c). However, upon introducing Co dopants the majority and minority E_g values were found as 0.72 eV and 0.31 eV, respectively. Thus, one can deduce that spin resolved band structure can clearly be observed in the presence of transition elements.

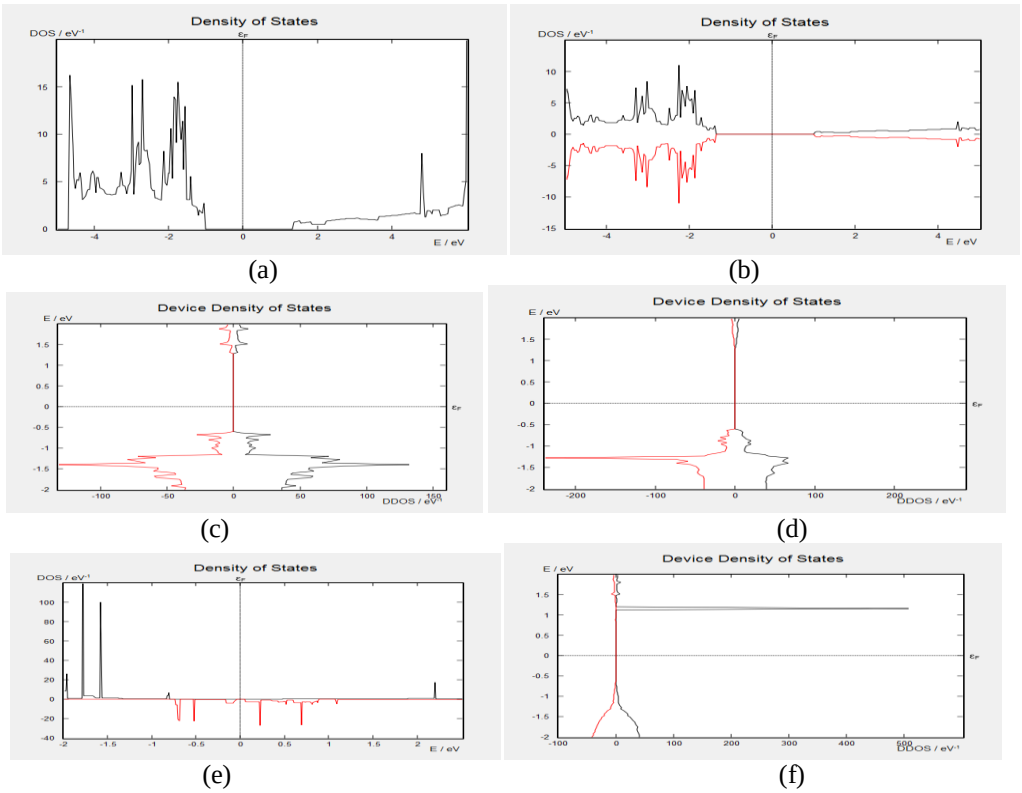

(a) (b)

(c) (d)

(e) (f)

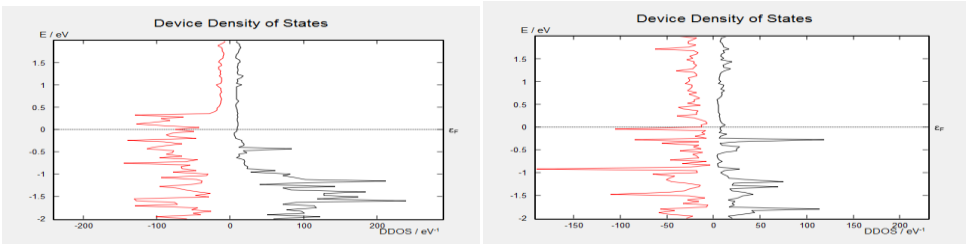

(g) (h)

Figure 5: Density of states in the absence of spin for (a) ZnO sheet and in the presence of spin for (b) ZnO sheet,(c) ZnO sheet device, (d) Distorted ZnO sheet device, (e) Co doped optimized ZnO sheet, (f) Co doped ZnO sheet device, (g) Ni-ZnO sheet device and (h) Ni-ZnO sheet device with U correction.

Figure 5, illustrates the DOS spectra for ZnO sheets in the form of periodic (bulk system) and device structures (open system). The default k-points in the calculations for periodic and device structures are (6,6,6) and (6,6,100), respectively. Thus a result without mentioning k-points means k-points sampling of (6,6,6) for a bulk system and (6,6,100) for a two probe system. For periodic structures, the energy gap in the band structure corresponds to the zero states in the DOS spectra around the E_f. Figure 5a indicates the DOS spectrum for ZnO sheet when spin is not involved. The E_g value of 1.86 eV for this system can also be obtained using Fig.5a (see Figure 4a and 5a). From Figure 5b-c we see that majority (spin up) and minority (spin down) variations in DOS are identical, meaning they are spin symmetric. Thus, there is no spin dependent variation for the associated structures in Figure 5b-c and so majority DOS becomes equal to minority DOS. As for the structure in Figure 5d-h, majority DOS is different from minority one, and hence they exhibit spin asymmetry. It means one can observe the spin resolved variation due to Co doping (Figure 5e and Figure 5f) and spin polarized Ni electrodes (Figure 5g and Figure5h) as expected. Distortion in Figure 5d induces an intriguing peak in minority DOS at the energy E = 1.3 eV which results in a distinct behavior from the majority one at this specific energy only. We see that when Ni electrodes (Ni-ZnO device) replace the ZnO (ZnO device) ones the DOS spectra become drastically modified (compare Figure 5c and g). Moreover, introducing the U term gives additional modification in the DOS spectrum resulting from the correction of band gap (Fig.5h). Hence, in order to propose a spintronic device one needs both U correction and transition metals like Co or Ni to induce a spin polarization required in spintronics. In addition to DOS, we calculated the spin dependent zero bias conductance at the E_f for a few device structures. For the Ni-ZnO sheet device in Figure 5g, majority and minority conductance were found as 8.78×10^{-11} S and 2.82×10^{-12} S, respectively. Upon including the U term (Figure 5h) they became 1.71×10^{-12} S, and 6.07×10^{-15} S respectively, which is more accurate due to the induced Hubbard correction. Semiconducting property was clearly observed for pure ZnO sheets in Figure 5b-d. However, upon introducing Co doping and Ni electrodes, the corresponding structures in Figure 5e-h reveal a metallic property and show spin resolved conductance at zero bias.

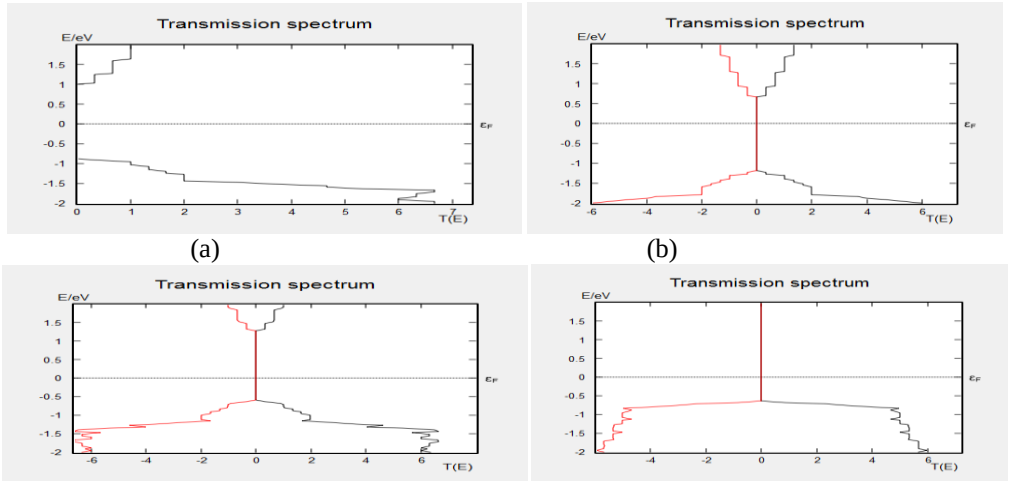

(a) (b)

(c) (d)

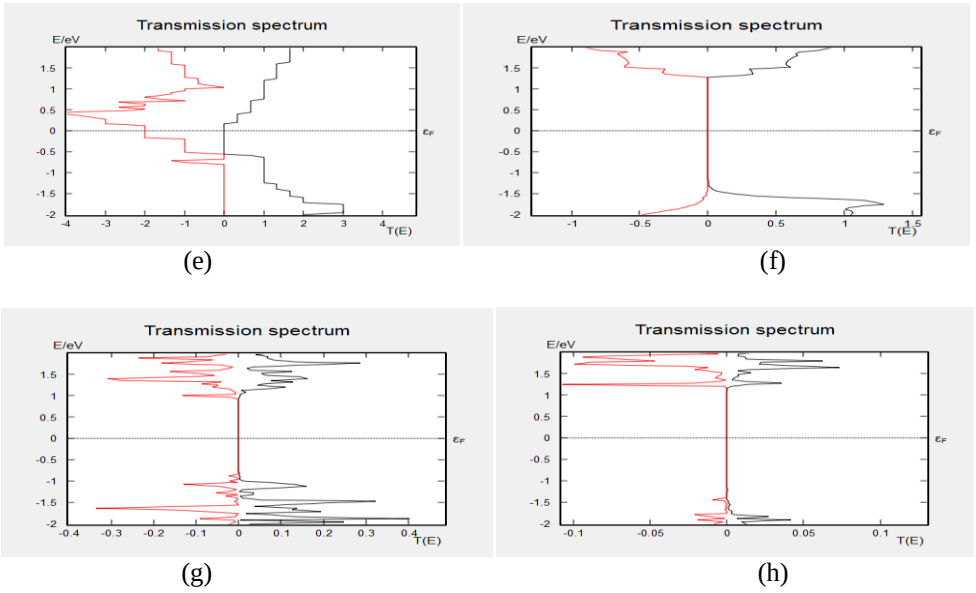

Figure 6: Transmission Spectrum in the absence of spin for (a) ZnO sheet and in the presence of spin for (b) ZnO sheet, (c) ZnO sheet device, (d) Distorted ZnO sheet device, (e) Co doped optimized ZnO sheet, (f) Co doped ZnO sheet device, (g) Ni-ZnO sheet device without U and (h) Ni-ZnO sheet device with U.

Figure 6, shows the T (E) of the systems mentioned in Figure 5. The zigzag variation in transmission for perfect system is a well know property as seen in Figure 6a and b [16]. In Figure 6a, the energy ranges, -1 eV to 1 eV, the zero transmittance means the energy of the electrons do not coincide with the transmission eigenvalues. It implies the semiconducting property which is also revealed in Figure 6b for both majority and minority electrons. In Figure 6b-d, majority and minority variations in the transmission spectra are identical, meaning they are spin symmetric. Thus, there is no spin dependent variation for the structures in Figure 6b-d as mentioned above. It was realized that the transmittance goes beyond unity in Figure 6b-d, which is related to transport channels in the bulk system for a periodic structure or central region for a device. If the number of transport channels is more than one, then one can obtain a transmission greater than one. The zero transmission range was – 0.5 eV to 1 eV and -1 eV to 1 eV for ZnO sheet device in Fig.5.4c and for distorted sheet device in Figure 6d, respectively. It means there is no electron transport from left electrode to right electrode in these specific energy intervals. Comparing Figure 6c and d, we see that distortion has a crucial effect on the transport. As for the transmittance in Figure 6e-h, majority transmission is different from the minority one, and hence they are spin asymmetric. It means there is a spin dependent variation due to Co doping (Figure 6e-f) and Ni electrodes (Figure 6g-h) as observed in DOS spectra in Figure 5e-h. Therefore in a pure perfect ZnO sheet we obtained that it is not possible to observe spin dependent transport and, so, one needs a transition metal like Co or Ni to induce a spin dependent property. It was observed that the transmission behavior was drastically modified when the electrodes are replaced by Ni ones (Figure 6g-h). We see that the transmittance shows step-like behavior especially for spin up electrons in Figure 6e. As shown in Figure 6e there is only spin down contribution to the transmission at the Fermi energy, resembling the half-metallic property. However both the spin up and down transmission in Figure 6f reveals a zero transmission in the energy range, -1.5 eV to 1 eV, implying a semiconducting property. Figure 6g and h illustrate the Ni-ZnO sheet device with and without U, respectively. The effect of U term is clearly observed in Figure 6h we see the increase in density of peaks in a certain energy interval due to the Ni electrodes some part of which is located in the central region. Semiconducting behavior was clearly realized for this device the observed region of zero transmission was in the energy range from -1 eV to 1 eV without U as seen in Figure 6g. Involving U term crucially modifies the transmission as shown in Figure 6h, where the zero transmission now occurs between -1.5 eV to 1 eV for both majority and minority electrons. In addition, we see the substantial reduction in the peaks of transmission in the presence of U. The number of peaks was also reduced especially for negative energies. Hence, the corresponding spin dependent transport can be revealed either by Ni electrodes or introducing transition metals in the central region. For a finite bias between the electrodes, the emerging spin dependent current can be controlled using spin polarized ferromagnetic electrodes or via playing the transition metal concentration together with its distribution throughout the central region.

4.2 Electronic Structural Properties of C Sheet

DFT results for Carbon sheets are presented with analysis and comparisons at each stage of a few different periodic and device structures. Here our aim is to present the electronic structure properties in order to make a comparison of ZnO and C based structures in terms of electronic transport behavior.

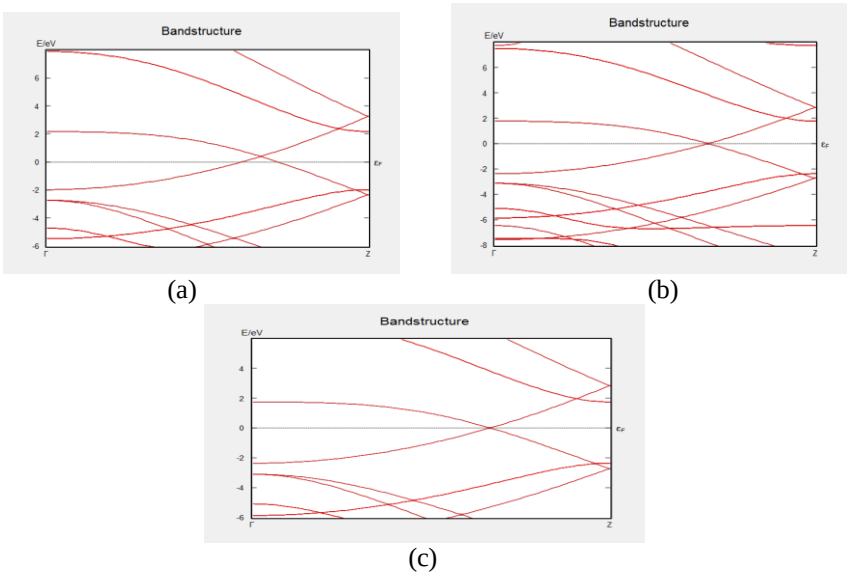

Figure 7: Band structures of C sheet. For (a) k point sampling of (6,6,6) with GGA, (b) k-point sampling of (15,15,15) with GGA, (c) k point sampling of (15,15,15) with LDA.

Figure 7, shows the band structures of C sheets in Figure 3a using the default k-point sampling of (6,6,6) and (15,15,15) with GGA together with LDA. Band structures are obtained to make a comparison between GGA (Figure 7a and b) and LDA (Figure 7c). K-point sampling is related to the accuracy and time taken for the calculations. We see a minute difference between Figure 7a with k points (6,6,6) and b with k points (15,15,15) under the GGA. It implies that k-point sampling of (6,6,6) is sufficient for this calculation without requiring high k-points which is time consuming. In this case, we can restrict our calculations employing the default k-point sampling (6,6,6). Besides, for the k points (15,15,15) we have also applied LDA to see the possible changes in the band structure (Figure 7c). As shown in Figure 7b and c, almost no changes were observed; meaning the DFT calculation with LDA becomes sufficient for this particular structure. From Figure 7, the metallic behavior is obvious, as the curves cross the Fermi level. Furthermore, the majority and minority variations in the band structures were identical, meaning they are spin symmetric. Thus, spin dependent behavior was not observed for the C sheet structure and, so majority E_g becomes equal to minority E_g.

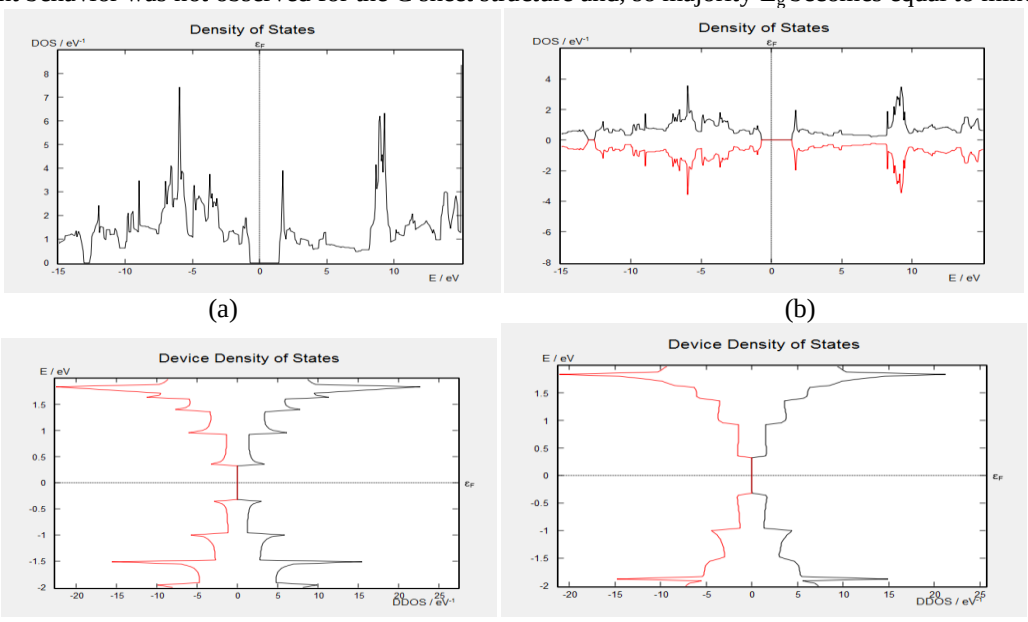

(c) (d)

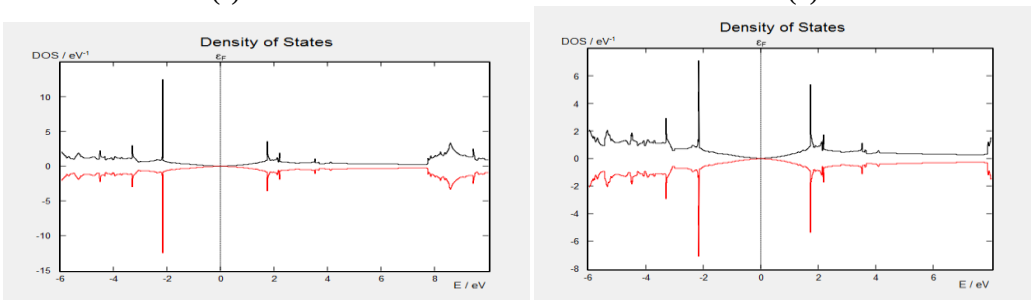

(e) (f)

Figure 8: Density of states for C sheet (a) in the absence of spin and (b) in the presence of spin. It is shown for (c) C sheet device and (d) Distorted C sheet device. Density of states for C sheet with k-point sampling of (15,15,15) (e) with GGA and (f) with LDA.

Figure 8, illustrates the DOS spectra for C sheets in the form of periodic and device structures. While, as mentioned above, the default k-point sampling in the calculations for periodic systems was (6,6,6), it was taken as (6,6,100) for the device structures due to open boundary conditions along the transport direction (from one electrode to the other one). Figure 8a indicates the DOS spectrum for C sheet when spin is not involved. From Figure 8b-f, we see that majority (spin up) and minority (spin down) variations in DOS are identical, meaning they are spin symmetric. Thus, there is no spin dependent variation or associated spin polarization for the structures in Figure 8b-f, and so majority DOS becomes equal to minority DOS. The semiconducting behavior was clearly observed for C based systems as shown in Figure 8. When spin is not involved, a well defined DOS peak at energy -6 eV and double peaks around 9 eV occurred (Figure 8a). Involving the spin induces intriguing peaks using the k point sampling (15,15,15) with GGA (Figure 8e) and LDA (Figure 8f), especially, at the energy -2 eV. Note the change in the peaks of DOS spectrum as a result of increasing k points and of LDA. For the C based device structure, the corresponding DOS spectra are shown in Figure 8c for perfect device and Figure 8d for distorted device. We see that there is an interesting variation in both majority and minority DOS, with perfect zigzag variation (Figure 8c). Besides, we realized peak intensity in the minority DOS at an energy E = 1.8 eV (Figure 8c). Moreover, we see that when distortion was considered (Figure 8d), there observed peak in minority DOS at same energy as in Figure 8c (E = 1.8 eV), but the zigzag variation in the DOS was drastically modified. Upon comparing Figure 8e and f at the same k-points sampling (15,15,15), we see that in both majority and minority DOS, we have peak at same energy E = 2 eV, and E = - 2 eV, respectively in both the structures (Figure 8e and f). But, the peak in the majority DOS in Figure 8f, were found to be much longer compare to the one in Figure 8e. However, realized an E_g value of 0.07 eV for the system in Figure 8e and f, which clearly revealed semiconducting behavior due to high k-points sampling (15,15,15).

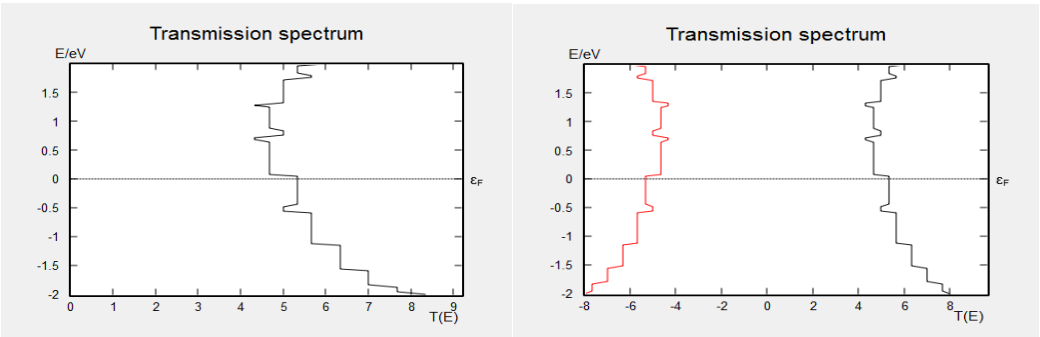

(a) (b)

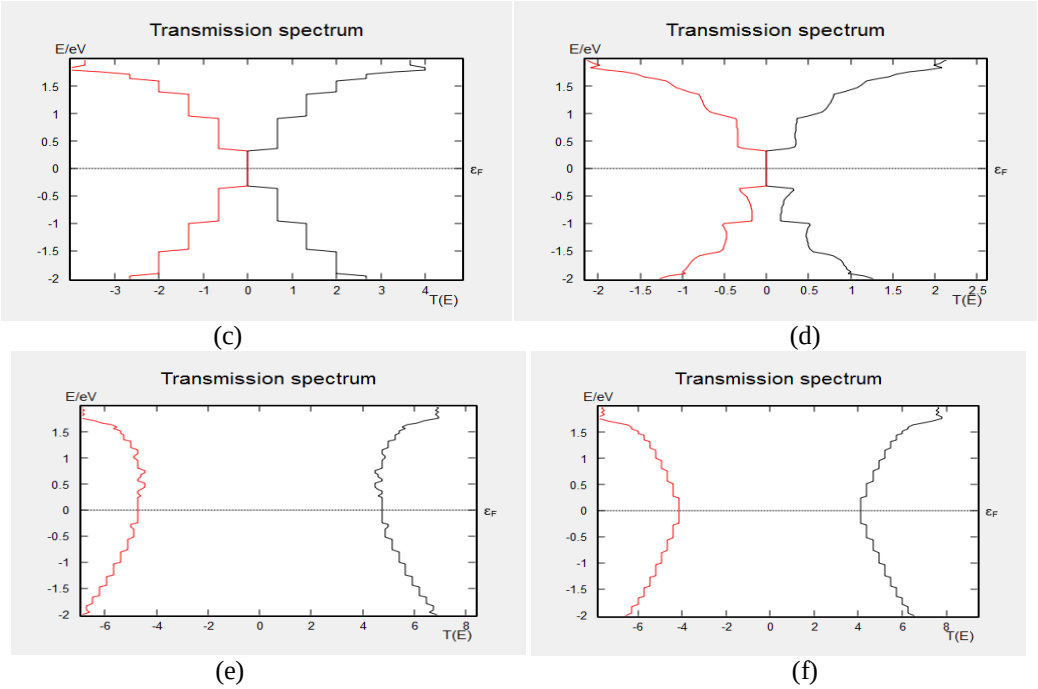

Figure 9: Transmission spectrum for C sheet (a) in the absence of spin and (b) in the presence of spin. It is shown for (c) C sheet device and (d) Distorted C sheet device. Transmission spectrum for C sheet with k-point sampling of (15,15,15) (e) with GGA and (f) with LDA.

Figure 9, shows the transmission spectra for the systems mentioned in Figure 8. As illustrated in this figure, the transmittance goes beyond the unity as a result of more than one transport channel in the periodic structure or central region of the C sheet device. The step-like variation in transmission for a perfect system is a well know property, which was observed in Figure 9a and b [16]. The step-like variation becomes perfect in the energy range, -0.5 eV to -2 eV when spin is not involved (Figure 9a). When spin is involved, transmission spectrum exhibited a spin-symmetric variation for C sheet without electrodes. Comparing Figure 9c and d, we see that distortion in C sheet device induces an effect on the transmission, as a result of which the step-like variation becomes distorted as expected. We observed that when the C sheet is located between the electrodes the transmission goes to zero at the Fermi energy, meaning no electron is transmitted from one electrode to the other one (Figure 9c and d). Increasing the k-points to (15,15,15) has a qualitative effect on the spectrum as the general behavior remains the same (Figure 9e). Using the LDA hardly modified the spectrum for the periodic C sheet structure as shown in Figure 9f. However the spectrum can be modified for a device structure.

4.3 Comparisons in Electronic Structural Properties of ZnO and Carbon Sheets

Some results for ZnO and C sheets are presented for the sake of comparisons when spin is involved. Thus, we explored differences and similarities of the electronic structural properties of these systems.

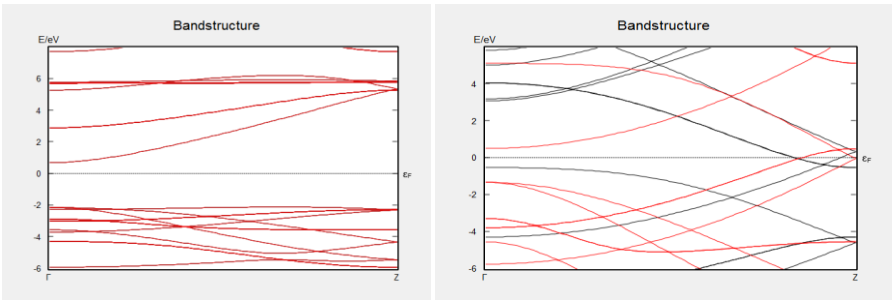

Figure 10: Band structures in the presence of spin with U correction for (a) ZnO sheet and (b) C sheet.

Figure 10, shows band structures of pure ZnO and C sheets when spin is involved. We see from Figure 10a that majority and minority variations in the band structures are identical with an energy gap, meaning

majority gap is the same as the minority one for a ZnO sheet. Thus, there is no spin dependent variation for the ZnO sheet exhibiting a semiconducting property. The U correction term raised the E_g value to 2.80 eV. As for the C sheet in Figure 10b, it was observed that majority E_g is different from minority E_g, and hence the corresponding band structure is spin asymmetric. Besides, metallic property was clearly observed in the C sheet in Figure 10b, as the spin dependent curves were crossing the Fermi energy.

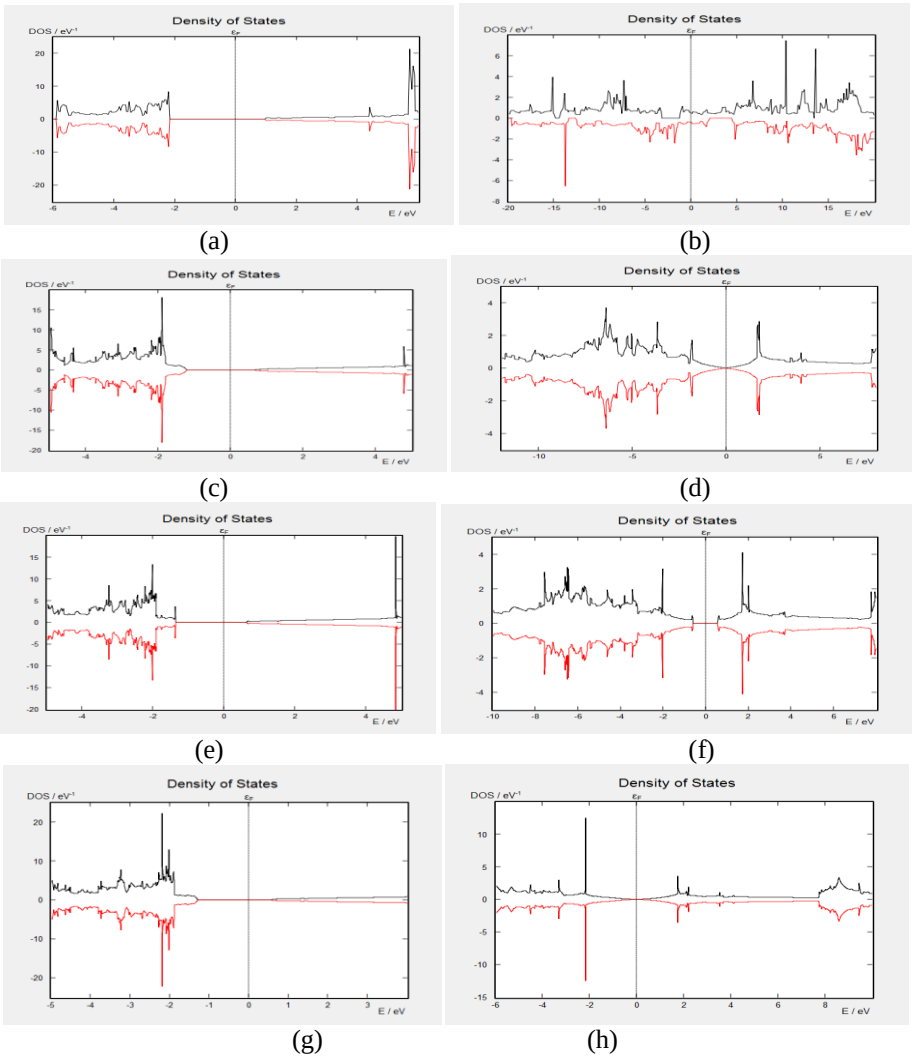

Figure 11: Density of states in the presence of spin with U term for (a) ZnO sheet and (b) C sheet. It is shown for ZnO sheet with k-points sampling (c) (9,9,9), (e) (12,12,12) and (g) (15,15,15). It is illustrated for C sheet with k-points sampling (d) (9,9,9), (f) (12,12,12) and (h) (15,15,15).

Figure 11, illustrates the DOS spectra for ZnO and C sheets when spin is involved. In addition to the default k-points (6,6,6) in the calculations, we also considered k-points sampling of (9,9,9) (Fig.5.10c and d), (12,12,12) (Figure 11e and f) and (15,15,15) (Figure 11g and h) so as to observe any changes that might affect the variations in the spectra obtained by k-points (6,6,6). For the ZnO sheet (Figure 11a, c, e, and g), the energy gap, due to the absence of states around the Fermi energy, is clearly seen in DOS spectra revealing spin symmetric behavior. Finite states are observed around the Fermi energy in the DOS spectra for the C sheet, even if they become close to zero upon increasing the k-points (Figure 11b, d, f and h). The intriguing point is that as a result of change in the k-points, we observed a transition from spin-asymmetric variation to spin-symmetric behavior for C sheet structures. While it is spin-asymmetric for the k-points (6,6,6), it becomes spin-symmetric for the higher k-points (Figure 11d, f and h). It implies the crucial role of k-points in DFT calculations. In Figure 11b, minority DOS at the energy -14 eV, and majority DOS at the energies 10 eV and 15 eV, show interesting peaks for the C sheet. The number and location of peaks changes as a consequence of k-points. For the ZnO sheet, these interesting peaks arise at the energy around -2 eV, which remains almost the same for the higher k-points. In addition, the qualitative behavior of the DOS spectra was hardly modified. Thus, the change in the k-points has almost no effect for the ZnO sheet structures.

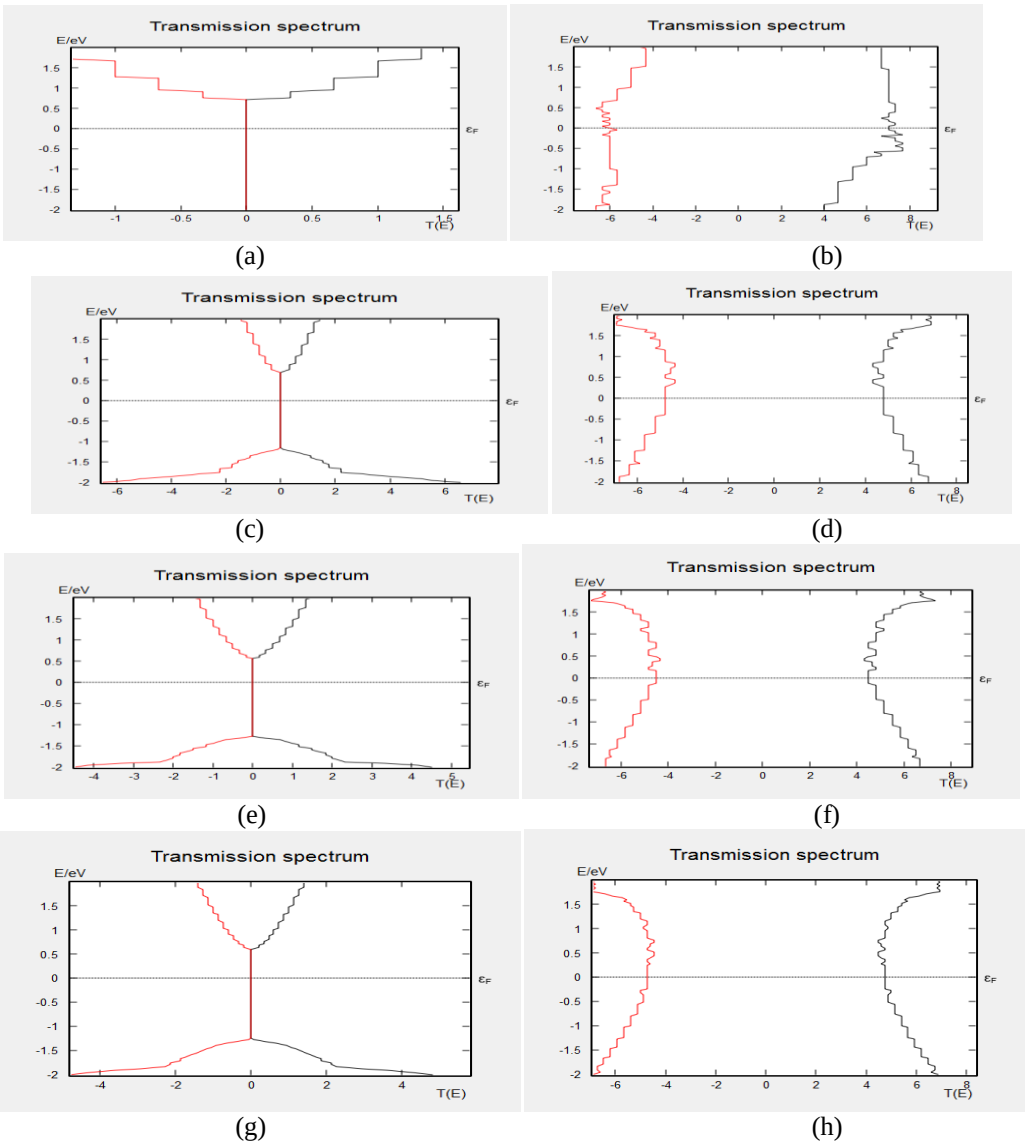

Figure 12: Transmission spectrum in the presence of spin with U term for (a) ZnO sheet and (b) C sheet. It is shown for ZnO sheet with k-points sampling (c) (9,9,9), (e) (12,12,12) and (g) (15,15,15). It is illustrated for C sheet with k-points sampling (d) (9,9,9), (f) (12,12,12) and (h) (15,15,15).

Figure 12, shows the transmission spectra of the systems mentioned in Figure 11 when spin is involved. As in the case of DOS spectra, in addition to the default k-points, we also considered k-points sampling of (9,9,9) (Figure 12c and d), (12,12,12) (Figure 12e and f) and (15,15,15) (Figure 12g and h). The step-like variation in all transmission spectra was observed, as expected. For the ZnO sheets, we see the spin-symmetric variation in the transmission. It becomes zero for a wide energy interval from -2 eV to 0.5 eV for k-points (6,6,6) shown in Fig.5.11a.This energy range becomes, -1.5 eV to 0.5 eV, for the higher k-points as illustrated in Figure 12c, e and g. The zero transmittance around the Fermi energy means that the energy of the electrons does not coincide with the transmission eigenvalues. It implies the semiconducting property. For the C sheet, as expected from the DOS spectra, a transition from spin-asymmetric (Figure 12b) transmission to spin-symmetric transmission (Figure 12d, f, and h) was observed as a result of increase in k-points. Thus we need to pay attention to the k-points in DFT calculations for C sheet structures. While for the ZnO sheet, the transmission variation was almost remained the same for the higher k-points (Figure 12a, c, and e). From the transmission spectra, zero bias and finite conductance at the Fermi energy are implied for ZnO and C sheet, respectively.

V. Conclusion And Recommendation

We theoretically examined ZnO and C sheets, as two dimensional systems, in the form of periodic and device structures to reveal the spin dependent electronic structure properties as well as spin dependent behavior together with magnetic properties. We mainly focused on ZnO sheets and, in addition, considered C sheets to make a comparison. We revealed similarities and differences between them in terms of electronic structure properties using some parameters. We also intended to expose the important role of Hubbard correction term and k-points on the spin dependent behavior. We employed the ATK software package for the calculations, which is based on DFT combined with NEGF. Various parameters and factors were considered, such as k-points sampling, exchange correlation, distortion, doping atom (Co) and Ni electrodes. Using the distortion, doping atom and Ni electrodes, we intended to observe the possible changes in the spin dependent behavior or spin polarization which is needed in developing spintronic devices. In order to be comparable to the experimental results and to mimic the realistic systems, systems were relaxed and distortions together with impurities were introduced. Ni and Co are ferromagnetic and transition metals which can induce magnetic moment or spin polarization in a system. In our case, Co atoms are added into the central region and Ni is used as a ferromagnetic electrode which provides spin polarized electrons during the electron transport. The results showed that the band structure becomes spin dependent for C sheets with a metallic property, while it has a spin independent energy gap for pure ZnO sheets. Especially, the band structure may crucially change as a consequence of U term and doping atoms. As expected, introducing the Co atoms yields in a spin dependent band structure for Co doped ZnO sheet. It resulted in a substantial change in the majority and minority energy gap relative to that for the pure ZnO sheet. Increasing the Co concentration reduces the energy gap and, so, it tends to transform the semiconducting property to metallic behavior. From the DOS and transmission spectra as well, we observed a spin symmetric variation for the pure ZnO sheet while for the pure C sheet it was spin asymmetric using the default k-points. We have observed an interesting behavior for the pure C sheet, for which a transition from spin-asymmetric variation to spin-symmetric behavior occurred when the k-point sampling was changed from the default one to higher k-points. It implies the crucial role of k-points in DFT calculations for the C sheet structures. However, for the pure ZnO sheet, the change in the k-points hardly modified the spectra.

Besides, the following notes are highly recommended for the accurate and reliable results in these kinds of calculations;

- For the realization of these systems (ZnO and C sheets), we deeply recommend that impurities, distortions etc. should be introduced before carrying out the calculations.
- However, introducing transition elements (especially Nickel or Cobalt atom) are needed for the spin polarized transport and induced magnetic moment to reveal the magnetic property.

Acknowledgement

The authors are grateful to management and staffs of Physics Laboratory, Fatih University Buyucekmece, Istanbul Turkey where all the simulation works of this manuscript was performed.

References

[1]. S.A. Wolf, D.D. Awschalom, R.A. Buhrman, J.M. Daughton, S. von Molnar, M.L. Roukes, A.Y. Chtchelkanova, D.M. Treger, "Spintronics: a spin-based electronics vision for the future", Science, Vol.; 294, pp;1488-1495, 2001.
[2]. G.A. Prinz, "Magnetoelectronics Applications", Science Campass, Vol.; 282, pp; 1660-1663, 1998.
[3]. H.X. Tang, F.G. Monzon, R. Lifshitz, M.C. Cross, and M.L. Roukes, "Ballistic spin transport in a two-dimensional electron gas", physical Review B, Vol.; 61, pp; 4437-4440, 2000.
[4]. F. Mireles and G. Kirczenow, "Coherent Spin Valve Phenomena and Electrical Spin Injection in Ferromagnetic/Semiconductor/Ferromagnetic Junction", Physical Reviview B, Vol.; 66, (214415), pp; 1-13, 2002.
[5]. T. Matsuyama, C.M. Hu, D. grundler, G. Meier, and U. Merkt, "Ballistic Spin Transport and Spin Interference in Ferromagnet/InAs(2DEG)/Ferromagnet Devices", Physical Review B, Vol.; 65, (155322), pp; 1-13, 2002.
[6]. Johnson, M. and Silsbee, R. H. "Interfacial charge-spin coupling: Injection and detection of spin magnetization in metals" Physical Review Letters, Vol. 55, pp; 1790-1793, 1985.
[7]. M.N. Baibich, J.M. Broto, A. Fert, F. Nguyen Van Dau, F. Petroff, P. Eitenne, G. Creuzet, A. Friederich, and J. Charzelas, "Giant Magnetoresistance of (001)Fe/(001)Cr Magnetic Superlattices" Physical Review Letters, Vol. 61, pp; 2472-2475, 1988.
[8]. G. Binasch, P. Grünberg, F. Saurenbach, W. Zinn, "Enhanced magnetoresistance in layered magnetic structures with antiferromagnetic interlayer exchange" Physical Review B, Vol. 39, (7), pp; 4828-4830, Doi:10.1103/PhysRevB.39.4828. 1989.
[9]. I. Zutic, J. Fabian, and S. D. Sarma, "Spintronics: fundamentals and applications" Reviews of Modern Physics, vol. 76, no. 2, pp. 323–410, 2004.
[10]. J. Fabian, A. Matos-Abiague, C. Ertler, P. Stano, and I. Zutic, "Semiconductor Spintronics" Acta Physica Slovaca, Vol. 57, no. 5, pp. 565-907, 2007.
[11]. Sarma, and Sankar Das., "Spintronics: A new Class of Device based on the Quantum of Electron Spin, rather than on Charge, may yield the next generation of Microelectronics." American Scientist, Vol., 89, pp; 516-523, 2001.
[12]. G. W. Burr, B. N. Kurdi, J.C. Scott, C.H. Lam, K. Gopalakrishnan, and R. S. Sheney, "Overview of candidate device technologies for storage-class memory" IBM Journal of Research and Development, Vol., 52, (4), pp; 449-464, Doi: 10.1147/rd.524.0449. 2008.
[13]. Q. Tang, Y. Li, Z. Zhou, C. Yongsheng and Z. Chen, "Tuning Electronic and Magnetic Properties of Wurtzite ZnO Nanosheets by Surface Hydrogenation" pubs.acs.org, Vol., 2 (8), pp; 2442-2447, Doi/abs/10.1021/am100467j, 2009.
[14]. S. Suzuki, T. Ariizumi, and Ming-Fang Li., "Mulliken Population Analysis of X-Ray Magnetic Circular Dichroism in Uranium

Monochalcogenides" Journal of the Physical Society Japan, Vol., 78 (7), pp; 305 - 8573, 2009.
[15]. R. C. Albers, N. E. Christensen, and A. Svane, "Hubbard-U band-structure methods" Journal of Physics: Condense Matter, Vol., 1, pp 10-28, arXiv: 0907.1028v1 [cond-mat.str-el], department of Physics and Astronomy, Aarhus University, Denmark, 2009.
[16]. A. Yipeng, J. Wei, and Z. Yang, "Z-like Conducting Pathways in Zigzag Graphene Nanoribbons with Edge Protrusions" Journal of Physical Chemistry, Vol., 116, issue 9, pp 5277-5980, State Key Laboratory of Surface Physics and Key Laboratory for Computational Physical Sciences (MOE) & Department of Physics, Fudan University, Shanghai 200433, China, 2012.